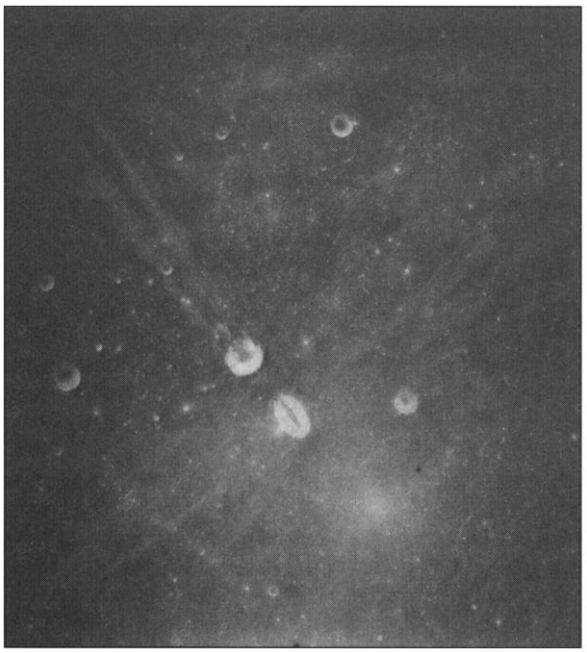

A rare event. The lunar craters Messier and Messier A are the only known example of a low-angle ricochet crater on the Moon. Messier, the elliptical crater, is 16.5 km long. Broad wings of ejecta extend perpendicular to the crater's axis, thrown out sideways as the meteorite grazed the Moon's surface. The bright streaks extend downrange and are probably composed of pulverized material shot out along the direction of motion. [Apollo 15 image AS15-2405(M).]

plains, where they are among the few solid rocks that accumulate on the surface. Similarly, most meteorite finds in the United States come from Kansas, which is covered by deposits of loess similar to the Pampas. On such plains, any stone is an oddity, and meteorites, while never common, are much more likely to be found.

The impact-produced glass is much harder to reconcile with this prosaic explanation. Bland *et al.* date the glass to about 500,000 years—much older than either the craters or the meteorites. The age of the Rio Cuarto glass is similar to ages reported for glass found in loess near the city of Necochea, nearly 800 km southeast of the Rio Cuarto site. Schultz also recovered very similar impact glasses about 500 km south of Rio Cuarto.

Impact glasses resembling those of Argentina are well known (*3*, *4*). Called tektites, these glassy stones are sometimes very beautiful and are often sold as gems. At present, four tektite strewn fields are recognized, three of which are associated with a known impact crater. The most famous is the Australasian field, which extends more than 10,000 km. It seems to be centered on Southeast Asia, but a source crater has not yet been identified. The Moldavite field is associated with the 22-km-diameter Ries Crater in Germany. The North American field was created by the recently discovered Chesapeake Bay crater (*5*); its diameter is controversial, but the entire structure is some 90 km in diameter. The Ivory Coast field was formed by the 10-km-diameter Bosumtwi crater in Ghana. The Moldavite and the Australasian tektites were created by impact melting of a surface layer of loess. Apparently the highly porous, silica-rich material of loess lends itself to strong heating by shock and readily forms glass.

Bland *et al.* propose that the Argentine glass is the product of a previously unrecognized impact somewhere near the Pampas. The size of the proposed Pampean tektite strewn field is intermediate between that of the Moldavite and the Australasian fields. Modeling of slightly oblique impacts, also reported in the paper, suggests that glass melted from the surface could have been splashed sufficiently far to account for the Argentine glasses.

Much work remains to be done to confirm the reality of this new tektite strewn field. More glass must be collected to better define the extent of the field. Furthermore, to qualify as a bona fide strewn field, all the glass must have the same age. The case would be stronger if a source crater of the same age could be found and the chemistry of the source rocks compared with the chemistry of the ejected glasses.

It does seem, however, that Bland *et al.* have cut the Gordian knot of the Pampas and revealed, not an oblique impact crater, but a much larger strewn field of tektites. As terrifying as the original picture of an oblique impact that scarred the Pampas a few thousand years ago was, the present view of a shower of hot glass over a region as large as Texas suggests a far more lethal event half a million years ago.

References

1. P. H. Schultz, R. E. Lianza, *Nature* **355**, 234 (1992).
2. P. A. Bland *et al.*, *Science* **296**, 1109 (2002).
3. J. A. O'Keefe, *Tektites and Their Origin* (Elsevier, New York, 1976).
4. S. R. Taylor, *Earth Sci. Rev.* **9**, 101 (1973).
5. C. W. Poag, *Sediment. Geol.* **108**, 45 (1997).

PERSPECTIVES: STRUCTURAL BIOLOGY

Not Just Another ABC Transporter

Amy L. Davidson

Gram-negative bacteria such as *Escherichia coli* have two protective membranes (outer and inner) that nutrients must traverse to reach the cytoplasm and nourish the cell. Small nutrients diffuse across the outer membrane into the periplasm through the water-filled pores of proteins called porins; meanwhile outer-membrane active transporters take up nutrients that are too big to squeeze through the porins (*1*). Once in the periplasm, substrate-specific transporters located in the inner membrane move nutrients into the cytoplasm. One class of these inner-membrane transporters, known as periplasmic binding protein–dependent transporters, belongs to the ATP-binding cassette (ABC) superfamily that couples ATP hydrolysis to active transport. These ABC transporter proteins operate in all species, from bacteria to human, mediating both uptake and efflux of a diverse array of compounds. A variety of human diseases, such as cystic fibrosis and macular degeneration, have been traced to defects in the genes encoding ABC transporters (*2*). On page 1091 of this issue, Locher *et al.* (*3*) present a high-resolution (3.2 Å) structure of the *E. coli* ABC transporter, BtuCD, that is responsible for transporting vitamin B_{12} into the cytoplasm of this bacterium (see the top figure). Their work contributes substantially to our understanding of the molecular mechanism of transport in this family.

The structure of the B_{12} transporter is the second high-resolution structure of a "complete" ABC transporter—that is, one containing two membrane-spanning domains or subunits (BtuC) and two ATP-binding cassettes (BtuD)—to be determined. (Six other cassettes have been crystallized in the absence of the membrane-spanning regions.) The first com-

The author is in the Department of Molecular Virology and Microbiology, Baylor College of Medicine, Houston, TX 77030, USA. E-mail: davidson@bcm.tmc.edu

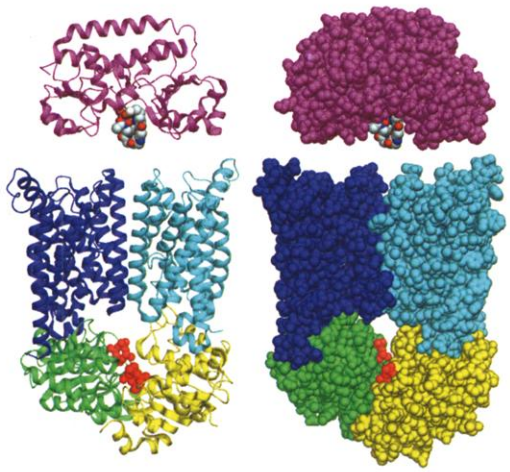

The ABC of transport. A structural study of the vitamin B_{12}-specific ABC transporter of *E. coli* (*3*) reveals a tetrameric protein comprised of two alpha-helical transmembrane subunits (blue and cyan) and two cytoplasmic ATP-binding cassettes (green and yellow). Two ATP-binding sites, located along a dimer interface, are occupied by tetravanadate (red). Also shown is a periplasmic binding protein (pink), bound to its substrate (gray), that is about to dock with the transporter to initiate translocation of the substrate into the cytoplasm. In this illustration, the ferric siderophore binding protein FhuD (*13*) substitutes for the B_{12} binding protein, whose structure has not yet been determined.

plete structure to be solved was that of MsbA, a protein thought to transport lipid A across the inner membrane of *E. coli* from its site of synthesis in the cytoplasm to its final destination in the outer membrane (*4*). Even a cursory inspection reveals substantial differences between BtuCD and MsbA. Whereas the membrane-spanning region of the MsbA dimer consists of two tidy bundles of six transmembrane α helices, each BtuC subunit contains 10 transmembrane helices that pack in an intricate fashion, crossing at different angles and sometimes breaking formation before reaching the opposite face of the membrane. The structure of BtuCD reveals a translocation channel positioned between the subunits that is large enough to accommodate B_{12} (*3*). The channel is gated closed at the cytoplasmic surface by two of the cytoplasmic loops that connect the transmembrane α helices. ABC transporters that move smaller nutrients across the membrane are predicted to have only 10 to 14 transmembrane helices, with 12 being the canonical number. This implies that the 20 helices seen in BtuCD may be needed to stabilize a larger central channel.

In contrast to the transmembrane structures, each of the eight available ATP-binding cassette structures has essentially the same fold irrespective of the nature of the transported substrate (*5*). In addition, the area of contact between the cassette and transmembrane region is the same in both MsbA and BtuCD. ATP hydrolysis by ABC transporters is highly cooperative, but how the two ATP-binding cassettes interact with each other remains controversial. In the first structure of an ATP-binding cassette (*6*)—that of HisP, a subunit of the bacterial histidine permease—the nucleotide-binding sites, as defined by the Walker A and B motifs (*7*), faced away from the HisP dimer interface. As a consequence, the bound ATP in HisP is exposed at the surface, in contrast to other ATPases where ATP is buried in a pocket. To rectify this inconsistency, Jones and George (*8*) provided an alternate model for dimerization of HisP. Their model proposed that the ABC family signature motif, Leu-Ser-Gly-Gly-Gln (LSGGQ), of each cassette completes the ATP-binding site of the opposing cassette such that the two ATP molecules are buried in the dimer interface. This would explain the strict requirement for two ATP-binding cassettes in each transporter, because residues from both cassettes would be required for hydrolysis of ATP. Supporting this model was the discovery of the same dimer interface in Rad50 (*9*), a distantly related ABC protein involved in DNA repair. However, none of the subsequent structures of true ABC transporters, including MsbA, have displayed this dimer interface, calling into question its relevance to the ABC transport mechanism.

The structure of BtuCD differs from the structure of MsbA and resembles that of Rad50 in that the LSGGQ motifs are again found opposite the ATP-binding motifs of the opposing subunits. Hence, this new structure of a bona fide ABC transporter shifts the balance of the controversy in favor of a common dimer interface for all ATP-binding cassettes in which the family signature or LSGGQ motif always participates in ATP binding and hydrolysis. If true, then it appears that the MsbA subunit, together with all isolated ATP-binding cassettes crystallized to date, have crystallized as monomers.

Structural alignment of BtuD, or any other ATP-binding cassette structure (*10*), with Rad50 reveals how ABC transporters might work. In figure 5 of the Locher *et al.* paper (*3*), we see that in the absence of ATP, the

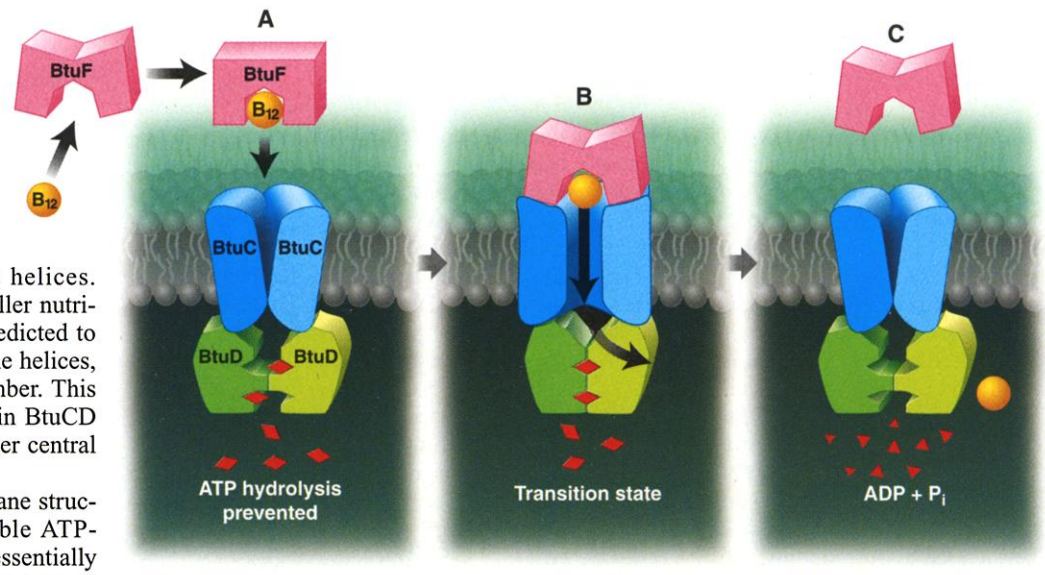

Releasing the grip on B_{12}. In the structure of the bacterial ABC transporter BtuCD (*3*), a B_{12} translocation pathway across the membrane (visible along the dimer interface of the BtuC subunits) is closed at the cytoplasmic surface. Conserved motifs from both BtuD subunits contribute to each of the ATP-binding sites. In the resting state, ATP hydrolysis is prevented because these motifs are held apart (**A**). The binding protein, BtuF, performs a dual role: It delivers B_{12} to the mouth of the transporter as it binds tightly to stabilize the transporter in the catalytic transition state conformation that promotes ATP hydrolysis (**B**). In this conformation, portions of the two BtuD subunits have moved together to complete the ATP-binding sites, BtuF has relinquished its grip on B_{12}, and rearrangements in the transmembrane helices have opened the translocation pathway from the binding protein to the cytoplasm. A vestibule located in the cytoplasm between the four subunits permits B_{12} to exit even while the BtuD subunits are still tightly engaged. After ATP hydrolysis and B_{12} release, the transporter returns to the original state and BtuF is released (**C**).

CREDIT: TOP, DOUGLAS C. REES; BOTTOM, KATHARINE SUTLIFF

LSGGQ motif of BtuD is pulled away from the Walker A motif of the opposing subunit by about 4 Å relative to the same motif in the Rad50 structure, where residues from both motifs make contact with bound ATP (*9*). Thus, activation of ATP hydrolysis may be associated with movement of the LSGGQ motif into contact with the phosphates of ATP (*11*). Likewise, release of ADP and/or P_i (inorganic phosphate) following hydrolysis may require the withdrawal of the LSGGQ motif (*10*). Because the two ATP-binding cassettes are tightly associated with the two transmembrane subunits, one can imagine that movement of the two cassettes relative to each other in response to ATP binding and hydrolysis could translate into movements that open the gate between the two transmembrane subunits, allowing B_{12} to enter the cytoplasm through the central channel (see the bottom figure).

This picture, however, is only partially complete. What prevents B_{12} from escaping back into the periplasm (leading to ATP hydrolysis without B_{12} transport)? Enter the periplasmic binding protein. Chen *et al.* (*12*) have recently shown that the periplasmic maltose binding protein is required for coupling maltose transport to ATP hydrolysis. In addition to binding the substrate with high affinity, the binding protein also stimulates ATP hydrolysis, becoming tightly bound to the transporter in the catalytic transition state, when ATP is trapped between the two subunits. Taking a cue from the maltose transport system (*12*), the tight binding interactions in the Btu system that are expected to develop during ATP hydrolysis—between the binding protein (BtuF) and the BtuC subunits, and between the BtuD subunits and ATP molecules along the dimer interface—may reduce the affinity of the binding protein for B_{12} as the gate opens to the cytoplasm. These simultaneous changes will allow B_{12} to dissociate and enter the cytoplasm, but not the periplasm, which is temporarily blocked by the physical presence of the binding protein BtuF in the transporter complex (see the bottom figure).

The BtuCD structure has a vestibule between the four subunits that appears large enough to allow release of B_{12} into the cytoplasm even while the ABC subunits are tightly engaged. A complex of transporter and binding protein resembling the catalytic transition state can be stabilized with phosphate analogs such as vanadate (*12*) or aluminum fluoride. Comparison of the ground state, as seen in the Locher *et al.* structure, with an intermediate resembling the catalytic transition state should elucidate the conformational changes that couple transport to ATP hydrolysis in an ABC transporter. Finally, the structural diversity of the transmembrane region documented by the first two structures of complete ABC transporters, each of which is tailored to do a specific job, underscores the importance of performing these experiments in many different ABC transporters to obtain a full understanding of how the energy of ATP hydrolysis can be harnessed to do work.

References

1. R. Koebnik, K. P. Locher, P. Van Gelder, *Mol. Microbiol.* **37**, 239 (2000).
2. M. Dean, Y. Hamon, G. Chimini, *J. Lipid Res.* **42**, 1007 (2001).
3. K. P. Locher, A. T. Lee, D. C. Rees, *Science* **296**, 1091 (2002).
4. G. Chang, C. B. Roth, *Science* **293**, 1793 (2001).
5. R. Gaudet, D. C. Wiley, *EMBO J.* **20**, 4964 (2001).
6. L. W. Hung *et al.*, *Nature* **396**, 703 (1998).
7. J. E. Walker, M. Saraste, M. J. Runswick, N. J. Gay, *EMBO J.* **1**, 945 (1982).
8. P. M. Jones, A. M. George, *FEMS Microbiol. Lett.* **179**, 187 (1999).
9. K. P. Hopfner *et al.*, *Cell* **101**, 789 (2000).
10. Y. R. Yuan *et al.*, *J. Biol. Chem.* **276**, 32313 (2001).
11. A. L. Davidson, *J. Bacteriol.* **184**, 1225 (2002).
12. J. Chen, S. Sharma, F. A. Quiocho, A. L. Davidson, *Proc. Natl. Acad. Sci. U.S.A.* **98**, 1525 (2001).
13. T. E. Clarke *et al.*, *Nature Struct. Biol.* **7**, 287 (2000).

PERSPECTIVES: RADIO GALAXIES

Bubbles, Flows, and Fields

A. C. Fabian

Most galaxies, including our own, appear to have a massive black hole at their center. Some, the active galactic nuclei, are visible to us as a result of luminous outpourings such as quasars and the less powerful Seyfert galaxies. About 10% of active galactic nuclei are strong radio emitters. Diametrically opposed pairs of powerful energetic jets squirt out of these "radio-loud" objects at relativistic speeds. The jets themselves are rarely detected; the strongest evidence for their existence may be a pair of lobes of radio-emitting material on either side of the nucleus where the jets are shocked and decelerated by surrounding gas.

The first of these jets was sighted by H. Curtis almost 90 years ago in the giant elliptical galaxy M87 in the Virgo cluster. Twin radio lobes were reported almost 50 years ago. Yet the matter content of jets (apart from the emitting electrons), their total power, and their evolution remain uncertain. The high spatial resolution x-ray imaging achieved by NASA's Chandra observatory is, however, beginning to answer these questions.

X-ray observations have proven so useful because the gaseous atmospheres that fuel the jets usually have temperatures on the order of 10^6 to 10^7 K. By studying the surrounding gas, particularly bubbles in the gas blown by the jets, their total power and history over the past 10^7 to 10^8 years can be deduced. Holes and depressions in the x-ray emission have now been seen around radio sources in numerous clusters, including the Virgo cluster, the Perseus cluster, Hydra A, and the Centaurus cluster (*1–5*).

The relativistic jets are believed to originate very close to the central black hole and are probably ejected up the rotation axis of the accreting gas, or the spin axis of the black hole itself. As the jet decelerates in the surrounding matter, a bubble of low-density heated gas and relativistic plasma accumulates about the end of the jet. Unless the jet is so powerful that it dominates the hot gas, the bubble expands until buoyancy forces cause it to rise up and break away as a new bubble forms. The situation is similar to that of a dripping tap, with relative densities and directions reversed.

A bubble appears as an x-ray hole because its density is low. Provided that the bubble is not expanding supersonically (which is unlikely because the x-ray images show no evidence for shocks), its pressure should be similar to that of the surrounding gas, which can be deduced from the x-ray data. Pressure is proportional to energy density, and the volume of the bubble therefore gives an estimate of its total energy. The age of the bubble can be derived from the buoyancy force, yielding the mean total power of the jets.

Alternatively, these quantities can be deduced from only the radio data. The pressure can be deduced, assuming that the total energy of the cosmic rays and magnetic field that produce the synchrotron radio emission is minimized. The age can be deduced by identifying a spectral break in the power-law spectrum due to synchrotron losses. The energy may not be at a minimum, however. Furthermore, the pressure associated with the positively charged particles presumed to accompany the radiating electrons has to be accounted for, as well as any other relativistic components that do not contribute to the observed waveband.

With standard parameters, this method

The author is at the Institute of Astronomy, University of Cambridge, Cambridge CB3 0HA, UK. E-mail: acf@ast.cam.ac.uk